Received: 23 May 2022 | Revised: 8 September 2022 | Accepted: 6 October 2022

DOI: 10.1002/zamm.202200222

ZAMM

ORIGINAL PAPER

Solution of variable-order partial integro-differential equation using Legendre wavelet approximation and operational matrices

Chetna Biswas[1] | **Subir Das**[1] | **Anup Singh**[2] | **Holm Altenbach**[3]

[1]Department of Mathematical Sciences, Indian Institute of Technology (BHU), Varanasi, India

[2]Department of Mathematics, Institute of Technology, Nirma University, Ahmedabad, Gujarat, India

[3]Faculty of Mechanical Engineering, Ottovon Guericke University Magdeburg, Magdeburg, Germany

Correspondence
Subir Das, Department of Mathematical Sciences, Indian Institute of Technology (BHU), Varanasi, India.
Email: sdas.apm@iitbhu.ac.in

Funding information
Board of Research in Nuclear Sciences, Grant/Award Number: 58/14/07/2022-BRNS/37041

This article is concerned with developing a method to find a numerical solution of a one-dimensional variable-order non-linear partial integro-differential equation (PIDE) viz., reaction–advection–diffusion equation with initial and boundary conditions. The proposed numerical scheme shifted Legendre collocation method is based on operational matrices. The operational matrices using one-dimensional wavelets are derived to solve the said variable-order model. First operational matrices have been introduced for integration and variable-order derivatives using one-dimensional Legendre wavelets (LWs). After that, using the shifted Legendre collocation points, the model is reduced to a system of algebraic equations, which are solved using Newton–Cotes method. The error is then calculated by comparing the numerical solution obtained from the system of algebraic equations and the known exact solution of an existing problem to validate the efficiency of the proposed numerical scheme. The main contribution of the article is the graphical exhibitions of the solution profile for different variable order derivatives in presence of different values of the parameters.

1 | INTRODUCTION

One of the crucial origins of fresh water is ground water, that fulfills our basic need for drinking water and also water for industries and agriculture. Groundwater provides about 97% of the fresh water on the earth that is why it is more important than surface water. Unfortunately, it is getting polluted because of direct or indirect discharge of pollutants into the water bodies. Main factors that are responsible for polluting water are industrialization, urbanization and agriculture. India stands in the list of countries affected by water pollution, that is why it is very important to develop a mathematical model to predict the movement of solute in aquifers and how it affects environment and human health. We require excellent understanding of chemical, physical and biological processes those can control solute transportation in ground water. We should definitely consider domain of problems, the parameters used to create groundwater model for field problems and also for the given boundary conditions. Researchers now a days are very much interested in the topic of solute transportation and that is why there are lots of methods found in recent years to solve several different models depicting solute transportation. Presently, many problems with different concepts of science are related with the non-linear equations [1–3]. During literature survey, various models on non-linear problems have been found [4–8]. Many dynamical systems when modeled, generate an integral term consisting of an unknown function. The integro-differential equations (IDEs) and the integral, appear in modeling due to several phenomena of sciences. An IDE is an equation that contains both integral and derivative of functions. This partial integro-differential equations (PIDEs) are advantageous in various applications, like, quantitative socio-dynamics [9–12]. Study of PIDEs has an uttermost powerful equations, which are fractional partial integro-differential equations (FPIDEs). In Liu and He [13], researchers have studied the fractional order thermoelastic problem of porous structure. In last few years, researchers have found the fractional calculus, as an efficient tool which can help one a lot in describing the behaviors of several dynamical systems with more accuracy. The PIDEs can be studied based upon Chebyshev wavelets, one-dimensional Legendre wavelets (LWs), cubic B-spline collocation, one-dimensional Bernoulli wavelets and so forth. Various studies are present in the literature to solve the variable-order differential equation (VODEs)[14] such as optimization method to solve variable-order Poisson equation, one-dimensional LWs to solve VO non-linear advection–diffusion equation with variable coefficients [15]. Countless natural systems can be shaped using fractional-order PDE, for example, pollution of groundwater. To model the transportation of pollutant in the surface water, atmosphere and groundwater, one can use the fractional order reaction–advection–diffusion equation (FRADE). The flow equations are non-linear, but advection and diffusion are of primary importance [16–19]. We are already familiar with the integer-order differentiation and integration whereas the integer-order differentiation and integration can be generalized with fractional calculus to an arbitrary order.

Recent years, there are a growth of important dynamical problems that depend on time, space or both and show behaviour of fractional order. In fact, variable-order calculus can be more useful for illuminating more complicated dynamical problems. Variable order operators are a new paradigm in science [20], have generalised the variable order case for Riemann–Liouville and Marchaud fractional integration and differentiation and also explained inversion formula. Different authors have explained different definitions for derivatives of variable order each suits the respective aim. Variable-order derivative is permitted to vary as a function of t or as a function of x or both. Researchers like Lorenzo and Hartley [21] have discovered deeper in the concept of variable-order derivative. For the Caputo-definition, Riemann–Liouville-definition, Marchaud-definition and Grünwald-definition, the researchers have suggested definitions based on variable-order operators. Operators with variable orders have kernels with variable exponents. This makes finding the analytical solutions for variable-order fractional differential equations more challenging. Fortunately, advancement of numerical techniques are at an early stage but can be more effective to find solutions. For the solution of VODEs, a consistent approximation is suggested [22]. Stability and convergence of finite-difference approximation are investigated for the variable-order non-linear fractional diffusion equation [23]. We can easily observe that variable-order operator is more effective when it comes for solving dynamical problems.

Porous media refers to a medium that contains pores. One of the primary elements for all the living things on earth is water, which is present in two forms on earth (underground, out of which only 2.5% is fresh) and surface water. Most important source of fresh water is underground water. Contaminated groundwater is very harmful to everyone – humans, wildlife, environment and so forth. The most of the structures through which contaminated ground water passes are porous type. Many scientists and researchers are working on predicting the movement of contaminated groundwater through several porous media through developing different models.

A lot of work has been done by so many researchers related to fractional-order diffusion equation[16, 24] to observe the nature of diffusivity of contaminated water in porous media. But to the best of the authors' knowledge, a very few works related to variable-ordered diffusion equation are found in the literature survey. In the present scientific contribution, the authors have considered one-dimensional variable-ordered non-linear partial differential equation. Main aim of this article is to achieve the numerical solution of the VOPIDE with higher accuracy. First, an operational matrix is introduced for variable-order derivative and another operational matrix for integration, which have been implemented for one-dimensional LWs to obtain the desired results. The VOPIDEs can be then, scaled down into a system of algebraic equations, by employing one-dimensional LWs approximations and the operational matrices for variable-order derivative and integration. After that Newton–Cotes collocation method is applied on the obtained system of algebraic equations to achieve the numerical solution of the VOPIDE using MATHEMATICA software (version 11.3).

2 | PRELIMINARIES

This section contains few definitions which have been used in the article.

2.1 | Definition

The fractional-order $\gamma(x, t)$ partial derivative of a function $w(x, t)$, with respect to x, in the Caputo sense [25–28] is defined as [29]

$$
{}_0^cD_x^{\gamma}w(x,t) = \begin{cases} \dfrac{1}{\Gamma(r-\gamma)}\int_0^x (x-\xi)^{r-\gamma-1}\dfrac{\partial^r w(\xi,t)}{\partial \xi^r}d\xi, & \text{if } r-1<\gamma<r, \\ \dfrac{\partial^r w(x,t)}{dx^r}, & \text{if } \gamma = r \in N. \end{cases} \tag{1}
$$

Similarly, with respect to t, the fractional-order $\gamma(x,t)$ partial derivative of a function $w(x,t)$ in the Caputo sense is

$$
{}_0^cD_t^{\gamma}w(x,t) = \begin{cases} \dfrac{1}{\Gamma(s-\gamma)}\int_0^t (t-\tau)^{s-\gamma-1}\dfrac{\partial^s w(x,\tau)}{\partial \tau^s}d\tau, & \text{if } s-1<\gamma<s, \\ \dfrac{\partial^s w(x,t)}{dt^s}, & \text{if } \gamma = s \in N, \end{cases} \tag{2}
$$

where $\gamma(x,t)$ represents a function of two variable x and t.

2.1.1 | Corollary

The Caputo derivative of VO-FD implies the following [29]:

$$
{}_0^cD_x^{\gamma}x^{\beta} = \begin{cases} \dfrac{\Gamma(\beta+1)}{\Gamma(\beta+1-\gamma)}x^{\beta-\gamma}, & \text{if } \beta \in N_0 \, and \, \beta \geq r, or \beta \notin N_0 \, and \, \beta > r, \\ 0, & \text{if } \beta \in N_0 \, and \, \beta < r, \end{cases} \tag{3}
$$

where $r-1<\gamma(x,t)\leq r$ and N_0 is the set of non-negative integers.

2.2 | The Legendre wavelets

This section consists of definitions of one-dimensional LWs. The LWs $\psi_{n,m}(t) = \psi^L(k,n,m,t)$ depend on four arguments, where $n = 1,2,\dots,2^{k-1}$, $k \in N$, $m = 0,1,\dots,(M-1)$, with m is the order of Legendre polynomial and t is the normalised time. LWs on interval [0,1] can be defined as

$$
\psi_{n,m}(t) = \begin{cases} \sqrt{m+\dfrac{1}{2}}2^{k/2}L_m(2^k t - 2n + 1), & \text{if } \dfrac{n-1}{2^{k-1}} \leq t \leq \dfrac{n}{2^{k-1}} \\ 0, & \text{Otherwise,} \end{cases} \tag{4}
$$

where

$$
\begin{aligned} L_0(t) &= 1, \\ L_1(t) &= t, \end{aligned} \tag{5}
$$

and

$$
L_{m+1}(t) = \frac{(2m+1)}{(m+1)}tL_m(t) - \frac{(m)}{(m+1)}L_{m-1}(t), m = 1,2,3,\cdots. \tag{6}
$$

2.3 | Approximation of a function

Approximation of a function $w(x,t) \in L^2[0,1]\times[0,1]$ can be written as

$$
w(x,t) \approx \Psi_{k,M}^T(t)W\Psi_{k_1,M_1}(x), \tag{7}
$$

where

$$\Psi_{k,M} = [\psi_{1,0}, \dots, \psi_{1,M-1}, \psi_{2,0}, \dots, \psi_{2,M-1}, \dots, \psi_{2^{(k-1)},0}, \dots, \psi_{2^{(k-1)},M-1}]^T,$$

$$\Psi_{k_1,M_1} = [\psi_{1,0}, \dots, \psi_{1,M_1-1}, \psi_{2,0}, \dots, \psi_{2,M_1-1}, \dots, \psi_{2^{(k_1-1)},0}, \dots, \psi_{2^{(k_1-1)},M_1-1}]^T,$$

and W is a $2^{k-1}M \times 2^{k_1-1}M_1$ coefficient matrix with entries as

$$w_{n,m,n_1,m_1} = \int_0^1 \psi_{n,m}(x)\left(\int_0^1 w(x,t)\psi_{n_1,m_1}(t)dt\right)dx. \tag{8}$$

3 | OPERATIONAL MATRICES

3.1 | The operational matrix for VO-FD

Let $\Phi(t)$ be a $2^{k_1-1}M_1$-dimensional column vector as

$$\Phi(t) = [\phi_1(t), \phi_2(t), \dots, \phi_{2^{k_1-1}M_1}(t)]^T, \tag{9}$$

where $\phi_i(t) = t^{i-1}$, $i = 1, 2, \dots, 2^{k_1-1}M_1$.

Then $\Phi(t)$ and the LWs vector $\Psi_{k_1,M_1}(t)$ are related as

$$\Phi(t) = R\Psi_{k_1,M_1}, \tag{10}$$

where $R_{i,j} = <\phi_i(t), \psi_j(t)>$.

3.1.1 | Lemma

Suppose $\Phi(t)$ be defined as in Equation (9) and $\gamma(x,t)$ $(0 < \gamma(x,t) \leq 1)$ be a positive real-valued function defined on R^2 [30]. Then the Caputo VO derivative of the order $\gamma(x,t)$ of $\Phi(t)$ can be represented as

$${}_0^cD_t^{\gamma(x,t)}\Phi(t) = F_t^{\gamma(x,t)}\Phi(t), \tag{11}$$

where $F_t^{\gamma(x,t)}$ is an operational matrix of order $2^{k_1-1}M_1 \times 2^{k_1-1}M_1$, given by

$$F_t^{\gamma(x,t)} = \frac{1}{t^{\gamma(x,t)}}\begin{pmatrix} 0 & 0 & \dots & 0 \\ 0 & \frac{\Gamma(2)}{\Gamma(2-\gamma(x,t))} & \dots & 0 \\ 0 & 0 & \dots & \vdots \\ \vdots & \vdots & \ddots & 0 \\ 0 & 0 & \dots & \frac{\Gamma(2^{k_1-1}M_1)}{\Gamma(2^{k_1-1}M_1-\gamma(x,t))} \end{pmatrix}. \tag{12}$$

3.1.2 | Theorem

Suppose $\Omega = [0,1] \times [0,1]$ and $\gamma(x,t)$ is a real-valued function with domain Ω [30]. The Caputo variable-order fractional derivative of Ψ_{k_1,M_1} of order $\gamma(x,t)$ is

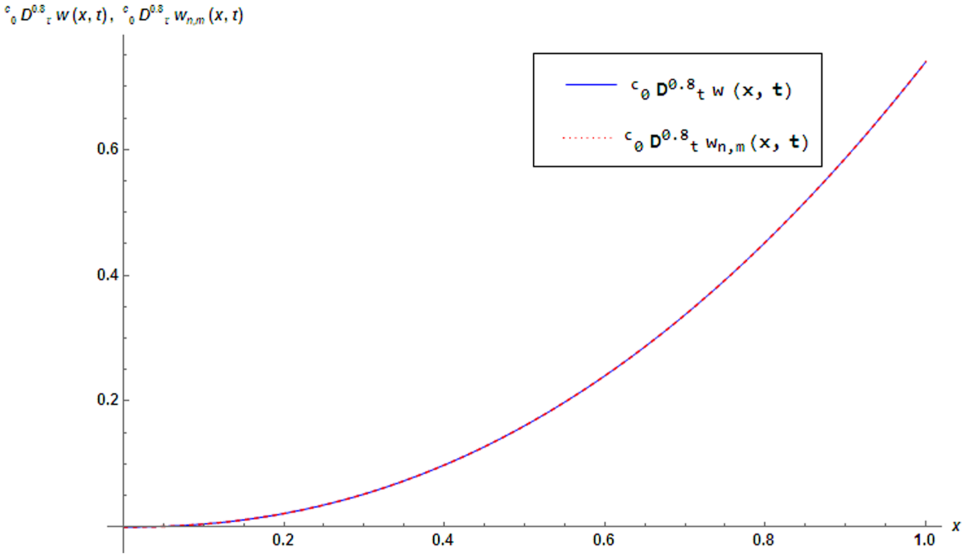

FIGURE 1 Plots of exact ${}^{c}_{0}D^{0.8}_{t}w(x,t)$ and approximate ${}^{c}_{0}D^{0.8}_{t}w_{n,m}(x,t)$ versus x at fixed $k = k_1 = 1, M = M_1 = 8$ and $t = 0.5$

$$ {}^{c}_{0}D^{\gamma(x,t)}_{t}\Psi_{k_1,M_1}(t) = (Q^{(\gamma(x,t))})\Psi_{k_1,M_1}(t), \tag{13}$$

where $Q^{(\gamma(x,t))} = R^{-1}F^{\gamma(x,t)}_{t}R$, R is $2^{k_1-1}M_1 \times 2^{k_1-1}M_1$ matrix defined in Equation (10) and $F^{\gamma(x,t)}_{t}$ is an $2^{k_1-1}M_1 \times 2^{k_1-1}M_1$ operational matrix defined in Equation (12).

Hence to find the approximate variable-order fractional derivative in Caputo sense of a function $w(x,t)$, first, find the approximation of the function $w(x,t)$ defined in Equation (7) as

$$ w(x,t) \approx \Psi^{T}_{k,M}(t)W\Psi_{k_1,M_1}(x) = w_{n,m}(x,t). \tag{14}$$

Now the approximation of variable-order derivative in Caputo sense using Equation (13) can be calculated as

$$ \begin{aligned} {}^{c}_{0}D^{\gamma(x,t)}_{t}w(x,t) &\approx {}^{c}_{0}\, D^{\gamma(x,t)}_{t}w_{n,m}(x,t) \\ &= Q^{(\gamma(x,t))}\Psi^{T}_{k,M}(t)F\Psi_{k_1,M_1}(x) \\ &= (R^{-1}F^{\gamma(x,t)}_{t}R)\Psi^{T}_{k,M}(t)F\Psi_{k_1,M_1}(x), \end{aligned} \tag{15}$$

Now let us verify the exact variable order Caputo derivative defined in Equation (3) with the approximated variable-ordered Caputo derivative defined in Equation (15). Figure 1 depicts the comparison of the exact with the approximated variable-ordered Caputo derivative of a function $w(x,t) = (xt)^{2.2}$ for order $\gamma(x,t) = 0.8$ at fixed $t = 0.5$.

3.2 | The operational matrix for partial derivative

Let $w_{n,m}(x,t)$ be the approximation of $w(x,t)$ as defined in Section 2.3, where $\Psi_{k_1,M_1}(t)$ is the LW column vector, then

$$ w_{n,m}(x,t) = \Psi^{T}_{k,M}(t)W\Psi_{k_1,M_1}(x), \tag{16}$$

where W is an unknown $2^{k_1-1}M_1 \times 2^{k_1-1}M_1$ order matrix. The derivatives can be approximated as [31]

$$ \frac{\partial w_{n,m}(x,t)}{\partial x} = \Psi^{T}_{k,M}(t)WD\Psi_{k_1,M_1}(x), \tag{17}$$

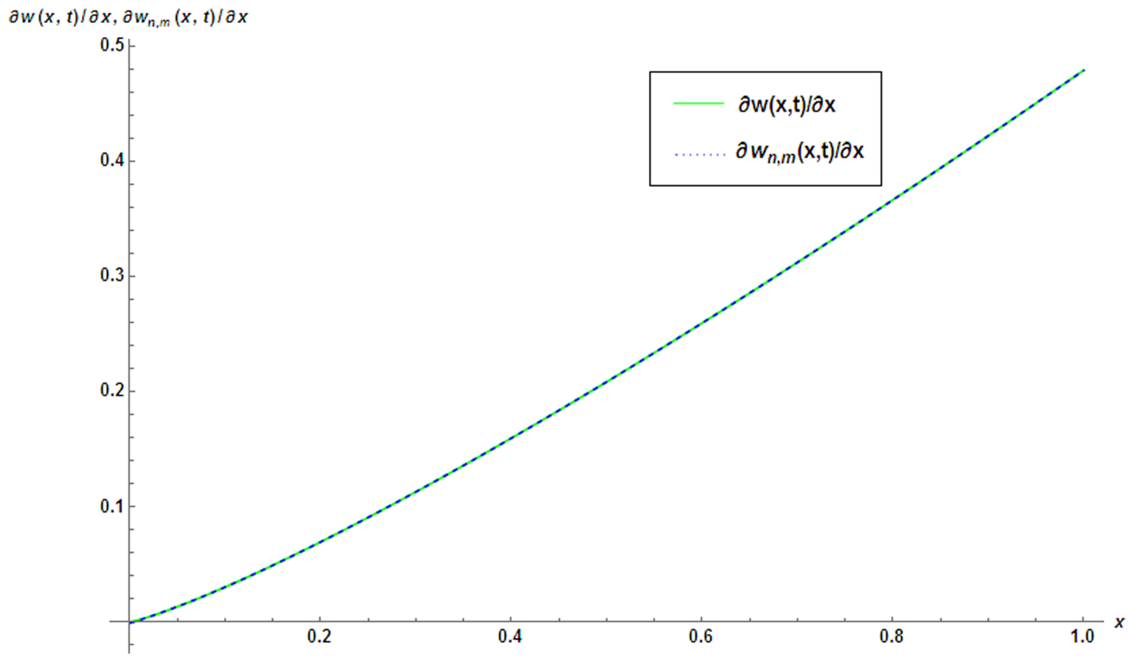

FIGURE 2 Plots of exact $\partial w(x,t)/\partial t$ and approximated $\partial w_{n,m}(x,t)/\partial t$ versus x at fixed $k = k_1 = 1$, $M = M_1 = 8$ and $t = 0.5$

where D is a $2^{k_1-1}M_1 \times 2^{k_1-1}M_1$ order operational matrix for derivative which is

$$D = \begin{pmatrix} F & 0 & 0 & \dots & 0 & 0 \\ 0 & F & 0 & \dots & 0 & 0 \\ 0 & 0 & F & \dots & 0 & 0 \\ \vdots & \vdots & \vdots & \ddots & \vdots & \vdots \\ 0 & 0 & 0 & \dots & F & 0 \\ 0 & 0 & 0 & \dots & 0 & F \end{pmatrix}, \tag{18}$$

in which F is a $M_1 \times M_1$ matrix with components

$$F_{r,s} = \begin{cases} 2^k\sqrt{(2r-1)(2s-1)}, & \text{if } r = 2, 3, \dots, M_1,\ s = 1, \dots, r-1, \text{ and } (r+s) \text{ is odd} \\ 0, & \text{Otherwise .} \end{cases} \tag{19}$$

For first-order derivative,

$$\frac{\partial w_{n,m}(x,t)}{\partial t} = \Psi^T_{k,M}(t) D^T W \Psi_{k_1,M_1}(x), \tag{20}$$

and for higher-order derivatives,

$$\frac{\partial^n w_{n,m}(x,t)}{\partial x^n} = \Psi^T_{k,M}(t) W D^n \Psi_{k_1,M_1}(x), \tag{21}$$

and

$$\frac{\partial^n w_{n,m}(x,t)}{\partial t^n} = \Psi^T_{k,M}(t) (D^T)^n W \Psi_{k_1,M_1}(x). \tag{22}$$

The verification of the approximated first-order partial derivative defined in Equation (20) with the exact first-order partial derivative of a function $w(x,t)$ with respect to x is given in Figure 2 taking the function as $w(x,t) = (xt)^{2.2}$ at fixed $t = 0.5$.

3.3 | Integral operational matrix

Let $\Psi_{k_1,M_1}(t)$ be the LW column vector defined in Section 2.3, then the integration of $\Psi_{k_1,M_1}(t)$ with respect to t can be defined as [32]

$$\int_0^t \Psi_{k_1,M_1}(\tau)d\tau = P\Psi_{k_1,M_1}(t), \tag{23}$$

where P is a $2^{k_1-1}M_1 \times 2^{k_1-1}M_1$ ordered matrix given by

$$P = \frac{1}{2^{k_1}}\begin{pmatrix} H & G & G & \dots & G & G \\ 0 & H & G & \dots & G & G \\ 0 & 0 & H & \dots & G & G \\ \vdots & \vdots & \vdots & \ddots & \vdots & \vdots \\ 0 & 0 & 0 & \dots & H & G \\ 0 & 0 & 0 & \dots & 0 & H \end{pmatrix}, \tag{24}$$

where G and H are $M_1 \times M_1$ ordered matrices given below:

$$G = \begin{pmatrix} 2 & 0 & 0 & \dots & 0 & 0 \\ 0 & 0 & 0 & \dots & 0 & 0 \\ 0 & 0 & 0 & \dots & 0 & 0 \\ \vdots & \vdots & \vdots & \ddots & \vdots & \vdots \\ 0 & 0 & 0 & \dots & 0 & 0 \\ 0 & 0 & 0 & \dots & 0 & 0 \end{pmatrix}, \tag{25}$$

and

$$H = \begin{pmatrix} 1 & \frac{1}{3^{1/2}} & \dots & 0 & 0 \\ -\frac{3^{1/2}}{3} & 0 & \dots & 0 & 0 \\ \vdots & \vdots & \ddots & \vdots & \vdots \\ 0 & 0 & .. & 0 & \frac{(2M_1-3)^{1/2}}{(2M_1-3)(2M_1-1)^{1/2}} \\ 0 & 0 & \dots & -\frac{(2M_1-1)^{1/2}}{(2M_1-1)(2M_1-3)^{1/2}} & 0 \end{pmatrix}. \tag{26}$$

Hence, we can define integration of function $w(x,t)$ as

$$\int_0^t w_{n,m}(x,\tau)d\tau = \Psi^T_{k,M}(t)(P^T)W\Psi_{k_1,M_1}(x). \tag{27}$$

The verification of the approximated integration defined in Equation (27) with the exact integration of a function $w(x,t)$ with respect to t is given in Figure 3 taking the function as $w(x,t) = (xt)^{2.2}$ at fixed $t = 0.5$.

4 | SOLUTION OF THE VARIABLE-ORDER NON-LINEAR PARTIAL DIFFERENTIAL EQUATION

In this section, a drive has been taken to solve the variable-order non-linear reaction–advection–diffusion equation given as

$${}_0^cD_t^{\gamma(x,t)}w(x,t) = D_1\frac{\partial^2 w(x,t)}{\partial x^2} + V_1\frac{\partial w(x,t)}{\partial x} + \lambda w(x,t)(1-w(x,t)) + \delta\int_o^t w(x,\tau)d\tau, \quad 0 \le \gamma(x,t) \le 1, \tag{28}$$

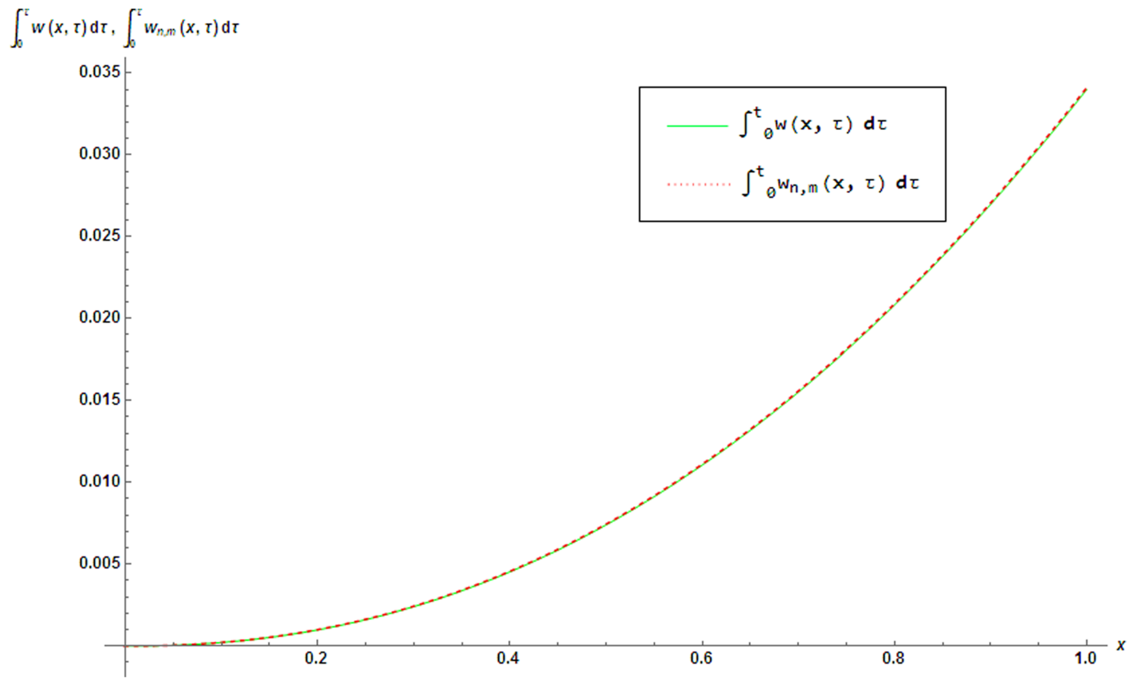

FIGURE 3 Plots of exact $\int_0^t w(x,\tau)d\tau$ and approximated $\int_0^t w_{n,m}(x,\tau)d\tau$ versus x at fixed $k = k_1 = 1$, $M = M_1 = 8$ and $t = 0.5$

under the initial and boundary conditions as

$$w(x,0) = \psi_1(x), \quad 0 \leq x \leq 1, \tag{29}$$

$$w(0,t) = \psi_2(t), \quad 0 \leq t \leq 1, \tag{30}$$

and

$$w(1,t) = \psi_3(t), \quad 0 \leq t \leq 1. \tag{31}$$

First, we will use shifted Legendre polynomial to approximate the function $w(x,t) \in [0,1] \times [0,1]$ as

$$w(x,t) \approx \Psi^T_{k,M}(t) W \Psi_{k_1,M_1}(x). \tag{32}$$

Then its derivatives can be defined as

$${}^c_0D_t^{\gamma(x,t)} w(x,t) \approx \left({}^c_0D_t^{\gamma(x,t)} \Psi^T_{k,M}(t)\right) W \Psi_{k_1,M_1}(x) = \Psi^T_{k,M}(t)\left(Q^{(\gamma(x,t))}\right)^T W \Psi_{k_1,M_1}(x), \tag{33}$$

$$\frac{\partial^n w(x,t)}{\partial x^n} \approx \frac{\partial^n \left(\Psi^T_{k,M}(t) W \Psi_{k_1,M_1}(x)\right)}{\partial x^n} = \Psi^T_{k,M}(t) W \frac{\partial^n \Psi_{k_1,M_1}(x)}{\partial x^n} = \Psi^T_{k,M}(t) W \left(D^n \Psi_{k_1,M_1}(x)\right), n \in N, \tag{34}$$

$$\int_0^t w(x,\tau)d\tau \approx \int_0^t \left(\Psi^T_{k,M}(\tau) W \Psi_{k_1,M_1}(x)\right)d\tau = \left(\int_0^t \Psi^T_{k,M}(\tau)d\tau\right) W \Psi_{k_1,M_1}(x) = \left(\Psi^T_{k,M}(t) P^T\right) W \Psi_{k_1,M_1}(x). \tag{35}$$

Now substituting Equations (33)–(35) in Equations (28)–(29), we get

$$\begin{aligned}\Psi^T_{k,M}(t)\left(R^{-1} F_t^{\gamma(x,t)} R\right)^T W \Psi_{k_1,M_1}(x) &= D_1 \Psi^T_{k,M}(t) W \left(D^2 \Psi_{k_1,M_1}(x)\right) + V_1 \Psi^T_{k,M}(t) W \left(D \Psi_{k_1,M_1}(x)\right) \\ &+ \lambda \Psi^T_{k,M}(t) W \Psi_{k_1,M_1}(x) - \lambda [\Psi^T_{k,M}(t) W \Psi_{k_1,M_1}(x)]^2 \\ &+ \delta \left(\Psi^T_{k,M}(t) P^T\right) W \Psi_{k_1,M_1}(x),\end{aligned} \tag{36}$$

and

$$\Psi^{T}_{k,M}(0)W\Psi_{k_1,M_1}(x) = \psi_1(x), \tag{37}$$

where $Q^{\gamma(x,t)} = R^{-1}F_t^{\gamma(x,t)}R$.

Equations (36) and (37) are rewritten as

$$\begin{aligned} H(x,t) = {} & \Psi^{T}_{k,M}(t)\left(R^{-1}F_t^{\gamma(x,t)}R\right)^{T} W\Psi_{k_1,M_1}(x) - D_1\Psi^{T}_{k,M}(t)W\left(D^2\Psi_{k_1,M_1}(x)\right) \\ & - V_1\Psi^{T}_{k,M}(t)W\left(D\Psi_{k_1,M_1}(x)\right) - \lambda(\Psi^{T}_{k,M}(t)W\Psi_{k_1,M_1}(x))(1-\Psi^{T}_{k,M}(t)W\Psi_{k_1,M_1}(x)) \\ & - \delta(\left(\Psi^{T}_{k,M}(t)P^{T}\right)W\Psi_{k_1,M_1}(x)) + \Psi^{T}_{k,M}(0)W\Psi_{k_1,M_1}(x) - \psi_1(x), \end{aligned} \tag{38}$$

and the boundary conditions (30) and (31) become

$$\Psi^{T}_{k,M}(t)W\Psi_{k_1,M_1}(0) = \psi_2(t), \tag{39}$$

$$\Psi^{T}_{k,M}(t)W\Psi_{k_1,M_1}(1) = \psi_3(t). \tag{40}$$

Equation (38) is collocated for $(m+1)\times(m+1)$ points at (x_i, t_j) and Equations (39) and (40) are collocated for $(m+1)$ points at t_j. Here x_i's are the roots of shifted Legendre polynomial $P^{l}_{m-1}(x)$ and t_j's are the roots of shifted Legendre polynomial $P^{\tau}_{m+1}(t)$. After the collocation of $(m+1)\times(m+1)$ points, we obtain a system of non-linear equations with $(m+1)\times(m+1)$ unknowns which are given as

$$\begin{aligned} H(x_i,t_j) = {} & \Psi^{T}_{k,M}(t_j)\left(R^{-1}F_t^{\gamma(x_i,t_j)}R\right)^{T} W\Psi_{k_1,M_1}(x_i) - D_1\Psi^{T}_{k,M}(t_j)W\left(D^2\Psi_{k_1,M_1}(x_i)\right) \\ & - V_1\Psi^{T}_{k,M}(t_j)W\left(D\Psi_{k_1,M_1}(x_i)\right) - \lambda\Psi^{T}_{k,M}(t_j)W\Psi_{k_1,M_1}(x_i)\left(1-\Psi^{T}_{k,M}(t_j)W\Psi_{k_1,M_1}(x_i)\right) \\ & - \delta\left(\Psi^{T}_{k,M}(t_j)P^{T}\right)W\Psi_{k_1,M_1}(x_i) + \Psi^{T}_{k,M}(0)W\Psi_{k_1,M_1}(x_i) - \psi_1(x_i), \end{aligned} \tag{41}$$

and

$$\Psi^{T}_{k,M}(t_j)W\Psi_{k_1,M_1}(0) - \psi_2(t_j) = 0, \tag{42}$$

$$\Psi^{T}_{k,M}(t_j)W\Psi_{k_1,M_1}(1) - \psi_3(t_j) = 0. \tag{43}$$

The system of non-linear equations are then solved by Newton–Cotes collocation points for $(m+1)\times(m+1)$ unknown entries of the unknown matrix W. The approximate solution $w_{n,m}(x,t)$ given by Equation (32) can be calculated using simple computation.

5 | NUMERICAL APPLICATION

In this section, the proposed method is applied on the following numerical example whose exact solution is known to validate the accuracy and efficiency of the method.

5.1 | Example [33]

$${}^{c}_{0}D_t^{\gamma(x,t)}w(x,t) + x\frac{\partial w}{\partial x} + \frac{\partial^2 w}{\partial x^2} = f(x,t) + \mu\int_0^t w(x,\tau)d\tau, \quad 0 < \gamma(x,t) \le 1, \tag{44}$$

TABLE 1 L_2-error between exact and approximate solutions at different values of t for $\gamma = 0.15, 0.35, 0.55, 0.75$ and 0.95

t	$\gamma = 0.15$	$\gamma = 0.35$	$\gamma = 0.55$	$\gamma = 0.75$	$\gamma = 0.95$
0.0625	2.17×10^{-2}	3.09×10^{-3}	6.30×10^{-5}	9.11×10^{-5}	6.63×10^{-6}
0.1875	5.39×10^{-3}	5.81×10^{-4}	5.53×10^{-5}	7.12×10^{-5}	5.07×10^{-6}
0.3125	3.31×10^{-3}	4.57×10^{-4}	1.37×10^{-5}	3.22×10^{-5}	4.77×10^{-6}
0.4375	1.34×10^{-3}	3.86×10^{-4}	5.41×10^{-5}	2.73×10^{-5}	2.07×10^{-6}
0.5625	4.68×10^{-4}	9.69×10^{-5}	4.01×10^{-6}	1.29×10^{-5}	1.02×10^{-6}
0.6875	2.92×10^{-4}	6.81×10^{-5}	2.94×10^{-6}	8.28×10^{-6}	8.23×10^{-7}
0.8125	1.01×10^{-4}	4.54×10^{-5}	1.82×10^{-6}	4.06×10^{-6}	5.62×10^{-7}
0.9375	4.70×10^{-5}	2.27×10^{-5}	1.12×10^{-6}	1.15×10^{-6}	2.48×10^{-7}

where

$$f(x,t) = 2t^{\gamma} + 2x^2 + 2 - \mu\left(x^2 t + \frac{2\Gamma(\gamma+1)t^{2\gamma+1}}{(2\gamma+1)\Gamma(2\gamma+1)}\right), \tag{45}$$

with initial condition

$$w(x,0) = x^2, x \in [0,1] \tag{46}$$

and boundary conditions

$$w(0,t) = \frac{2\Gamma(\gamma+1)t^{2\gamma}}{\Gamma(2\gamma+1)}, t \in [0,1] \tag{47}$$

and

$$w(1,t) = 1 + \frac{2\Gamma(\gamma+1)t^{2\gamma}}{\Gamma(2\gamma+1)}, t \in [0,1]. \tag{48}$$

The exact solution of the problem is given by [33]

$$w(x,t) = x^2 + \frac{2\Gamma(\gamma+1)t^{2\gamma}}{\Gamma(2\gamma+1)}. \tag{49}$$

For the comparison of the approximate solution with the exact solution, let us define the L_2- error as

$$L_2(t) = \sqrt{\int_0^1 |u(x,t) - u_{k,M,k_1,M_1}(x,t)|^2 dx}, \tag{50}$$

where $u(x,t)$ and $u_{k,M,k_1,M_1}(x,t)$ represent the exact and approximate solutions, respectively.

The proposed method is applied in the aforementioned example for $\mu = 1$, $k = k_1 = 1$, $M = M_1 = 7$ and $\gamma = 0.15, 0.35, 0.55, 0.75, 0.95$, just to get the approximate solution and the results of L_2-error are depicted through Table 1. Figure 4 depicts the absolute error $|w(x,t) - w_{num}(x,t)|$ between exact and approximate solutions versus x at fixed $t = 0.5$, whereas Figure 5 depicts the comparison between exact solution and the approximate solution of $w(x,t)$ for a fixed $t = 0.5$.

6 | NUMERICAL RESULTS AND DISCUSSION

After the validation of the efficiency and the accuracy of the derived scheme in the previous section, the proposed method is applied to solve the VOPIDE given in Equation (28) on domain [0,1] under the following prescribed initial and boundary conditions as

$$w(x,0) = 1, \quad 0 \le x \le 1, \tag{51}$$

$$w(0,t) = 0 = w(1,t), \quad 0 \le t \le 1. \tag{52}$$

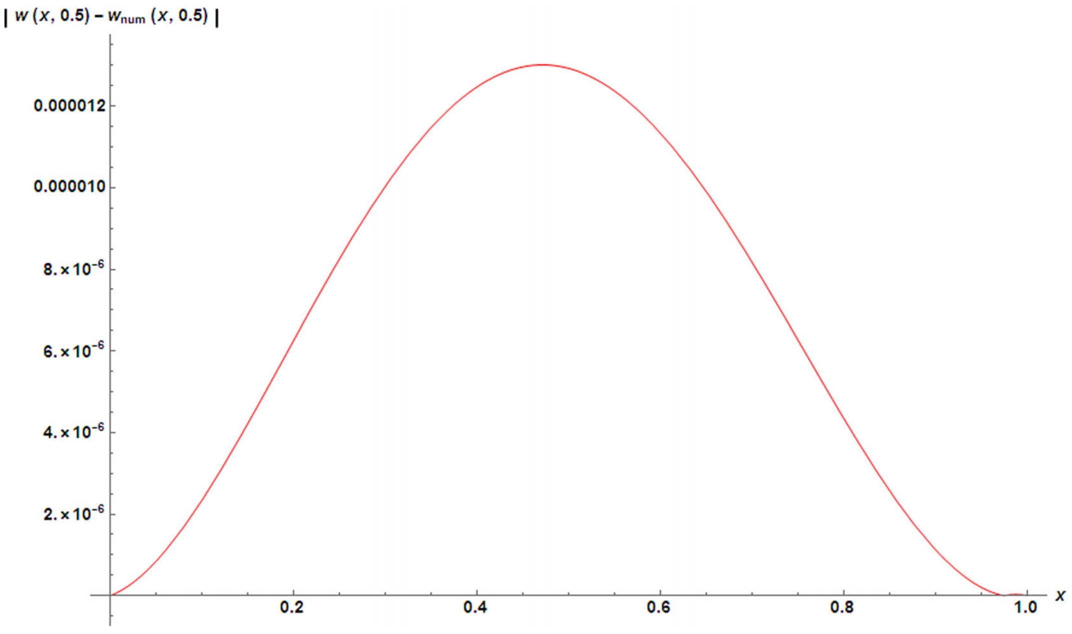

FIGURE 4 Plots of absolute error between exact and approximate solutions versus x at fixed $t = 0.5$

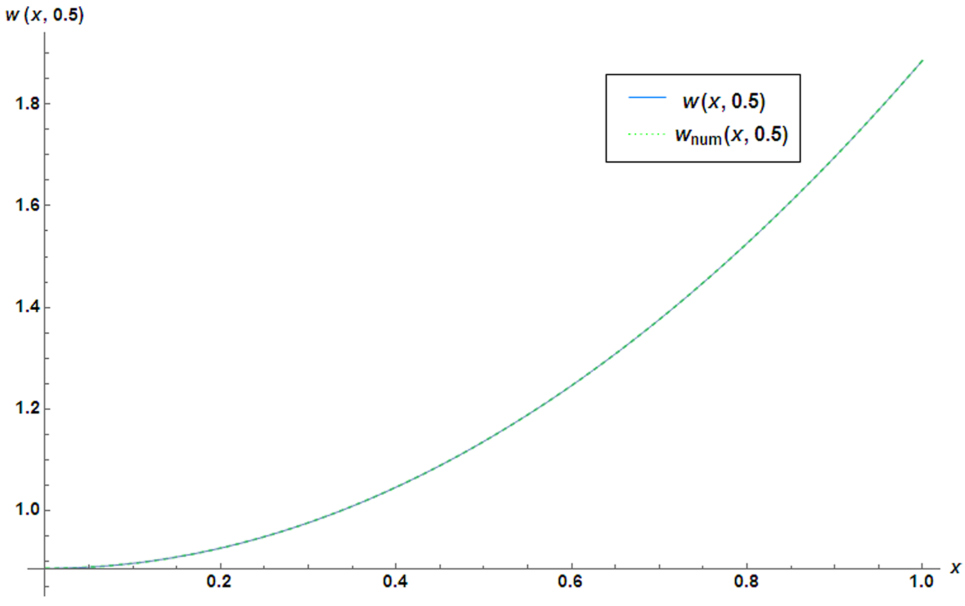

FIGURE 5 Plots of exact $w(x, 0.5)$ and approximate $w_{num}(x, 0.5)$ solutions versus x at fixed $t = 0.5$

The proposed scheme given in Section 3.1 is applied on the problem (28) under the conditions (51) and (52) to obtain a system of equations by Newton–Cotes collocation points. In Figure 6, we notice the variations of the solution when the parameters are considered as $\lambda = 1, \delta = 1, D_1 = 1, V_1 = 1$ and $\gamma(x,t) = xt, (xt)^2$ and $(x+t)/2$ at fixed $t = 0.5$.

Figure 7 provides the variations of the solution profile when $\lambda = 0, \delta = 1, D_1 = 1, V_1 = 1$ and $\gamma(x,t) = xt$ and $(x+t)/2$ at fixed $t = 0.5$. Whereas from Figure 8, it is noticed that the variations of the solution profile when the parameters are fixed as $\lambda = 1, \delta = 1, D_1 = 1, V_1 = 0$ and $\gamma(x,t) = xt$ and $(x+t)/2$ at fixed $t = 0.5$.

Figure 9 gives the variations of the solution when we fix $\lambda = 1, \delta = 0, D_1 = 1, V_1 = 1$ and $\gamma(x,t) = xt$ and $(x+t)/2$ at fixed $t = 0.5$ and Figure 10 shows the variations of the solution when $\lambda = 0, \delta = 0, D_1 = 1, V_1 = 0$ and $\gamma(x,t) = xt$ and $(x+t)/2$ at fixed $t = 0.5$.

Figure 11 provides the variations of the solution when we fix $\lambda = 0, \delta = 0, D_1 = 1, V_1 = 1$ and $\gamma(x,t) = xt$ and $(x+t)/2$ at fixed $t = 0.5$. Figure 12 depicts the variations of the solution when $\lambda = 1, \delta = 0, D_1 = 1, V_1 = 0$ and $\gamma(x,t) = xt$ and $(x+t)/2$ at fixed $t = 0.5$.

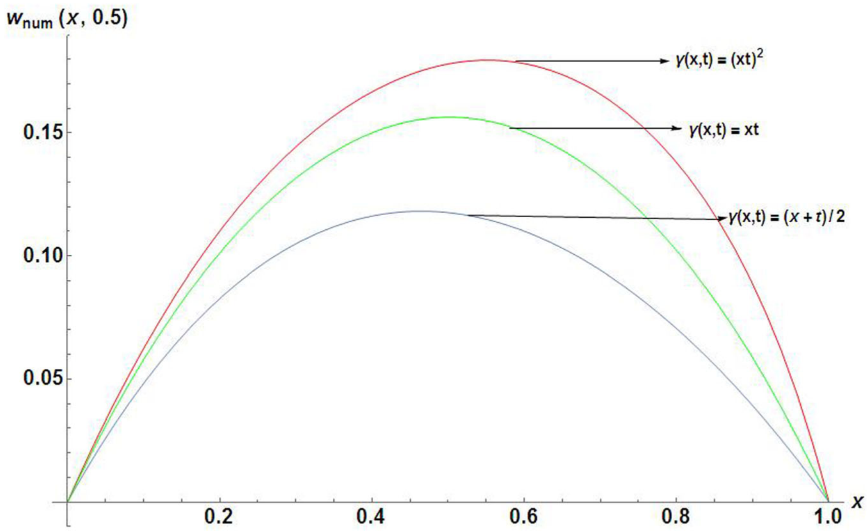

FIGURE 6 The plots of variation of the solution for the values of the parameters $\lambda = 1, \delta = 1, D_1 = 1, V_1 = 1$ and $\gamma(x,t) = xt$, $(xt)^2$ and $(x+t)/2$ at fixed $t = 0.5$

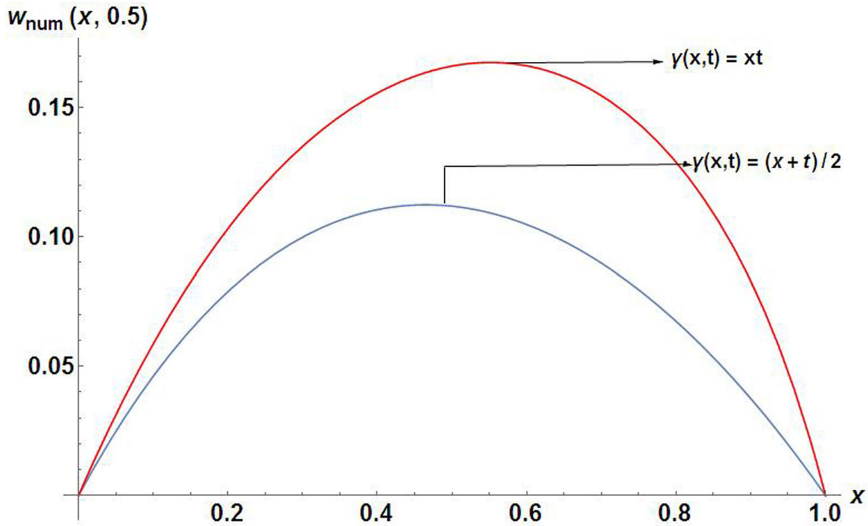

FIGURE 7 Plots of $w(x, 0.5)$ with $\lambda = 0$, $\delta = 1, D_1 = 1, V_1 = 1$ and $\gamma(x,t) = xt$ and $(x+t)/2$ at fixed $t = 0.5$

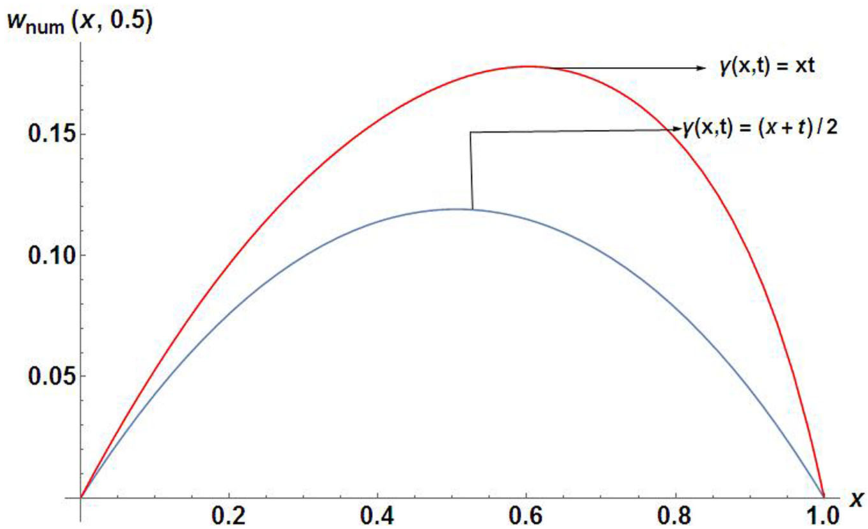

FIGURE 8 Plots of $w(x, 0.5)$ with $\lambda = 1$, $\delta = 1, D_1 = 1, V_1 = 0$ and $\gamma(x,t) = xt$ and $(x+t)/2$ at fixed $t = 0.5$

FIGURE 9 Plots of $w(x, 0.5)$ with $\lambda = 1$, $\delta = 0$, $D_1 = 1$, $V_1 = 1$ and $\gamma(x,t) = xt$ and $(x+t)/2$ at fixed $t = 0.5$

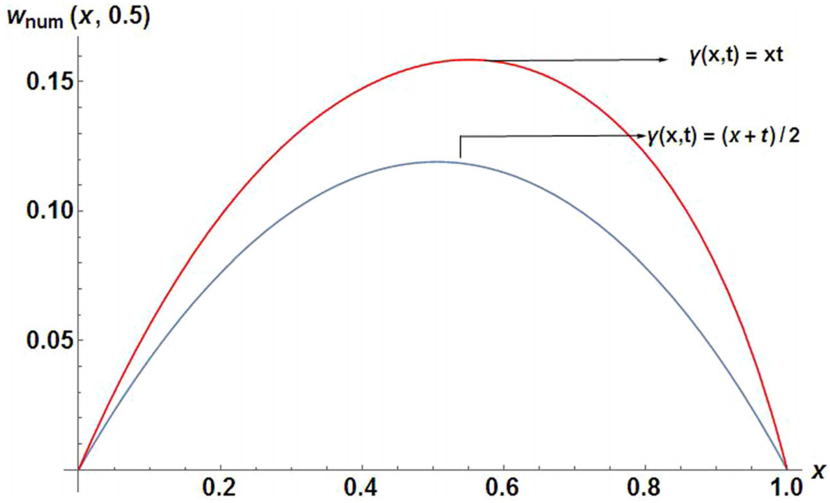

FIGURE 10 Plots of $w(x, 0.5)$ with $\lambda = 0$, $\delta = 0$, $D_1 = 1$, $V_1 = 0$ and $\gamma(x,t) = xt$ and $(x+t)/2$ at fixed $t = 0.5$

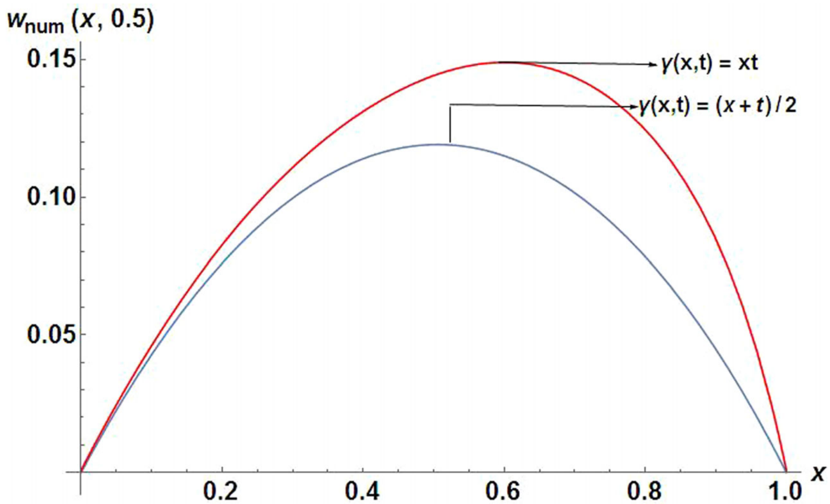

FIGURE 11 Plots of $w(x, 0.5)$ with $\lambda = 0$, $\delta = 0$, $D_1 = 1$, $V_1 = 1$ and $\gamma(x,t) = xt$ and $(x+t)/2$ at fixed $t = 0.5$

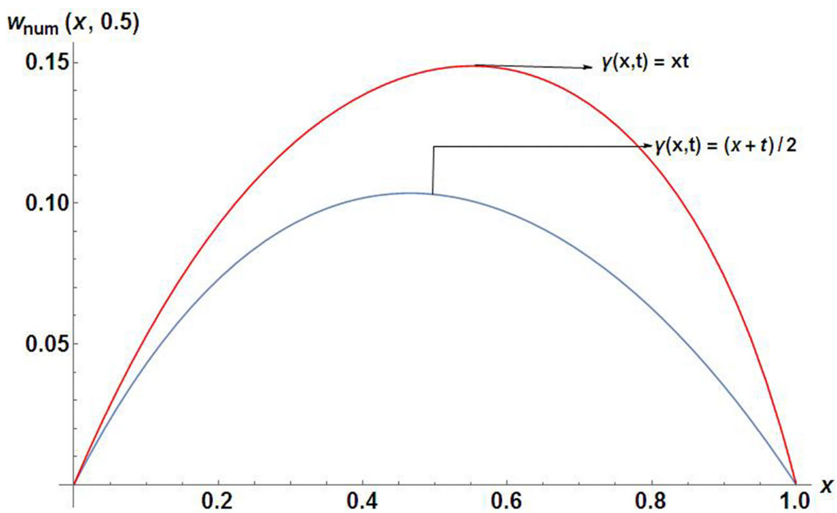

Figures 13 and 14 show that variations of $w(x,t)$ versus x for the values of parameters $\lambda = 1$, $\delta = 1$, $D_1 = 1$, $V_1 = 1$ and $\gamma(x,t) = xt$ and $(x+t)/2$ at fixed $t = 0.5$ and $\lambda = 0$, $\delta = 1$, $D_1 = 1$, $V_1 = 0$ and $\gamma(x,t) = xt$ and $(x+t)/2$ at fixed $t = 0.5$, respectively.

We observe from Figures 6–14 that the solute concentration diffuses lesser for the case of linear order as compared to that of non-linear order.

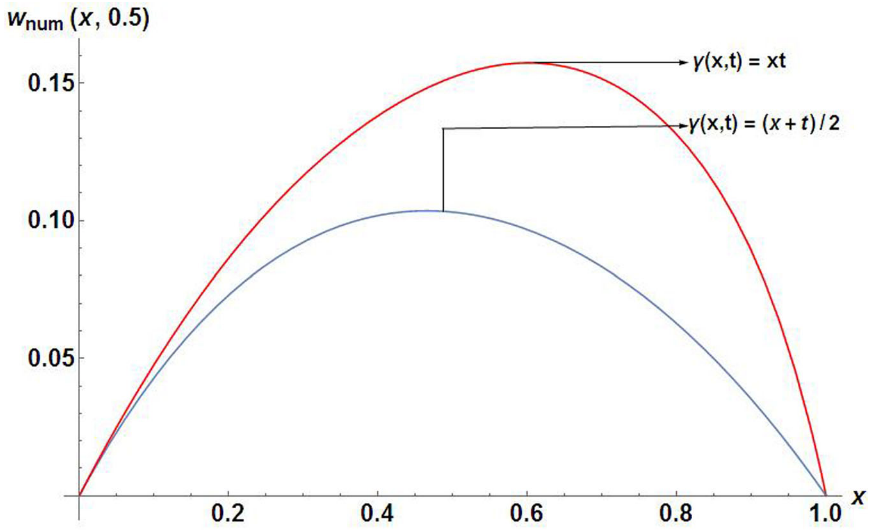

FIGURE 12 Plots of $w(x, 0.5)$ with $\lambda = 1, \delta = 0, D_1 = 1, V_1 = 0$ and $\gamma(x, t) = xt$ and $(x + t)/2$ at fixed $t = 0.5$

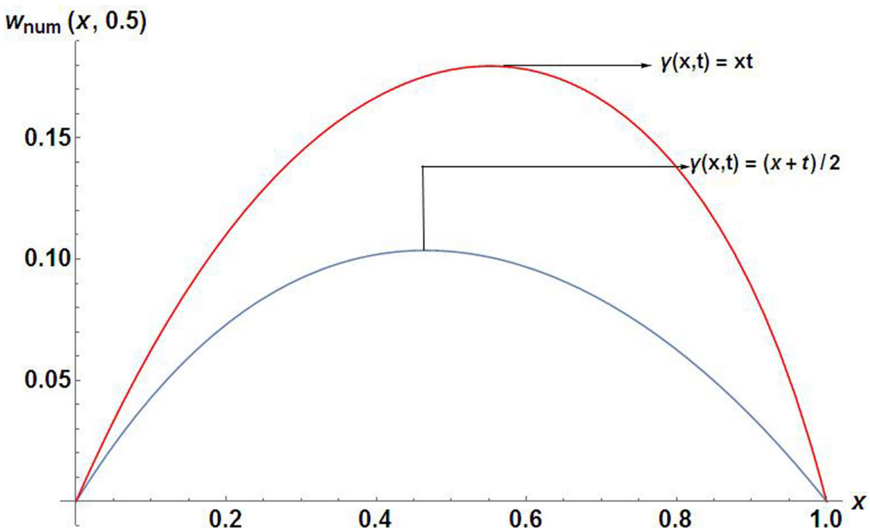

FIGURE 13 Plots of $w(x, 0.5)$ with $\lambda = 1, \delta = 1, D_1 = 1, V_1 = 1$ and $\gamma(x, t) = xt$ and $(x + t)/2$ at fixed $t = 0.5$

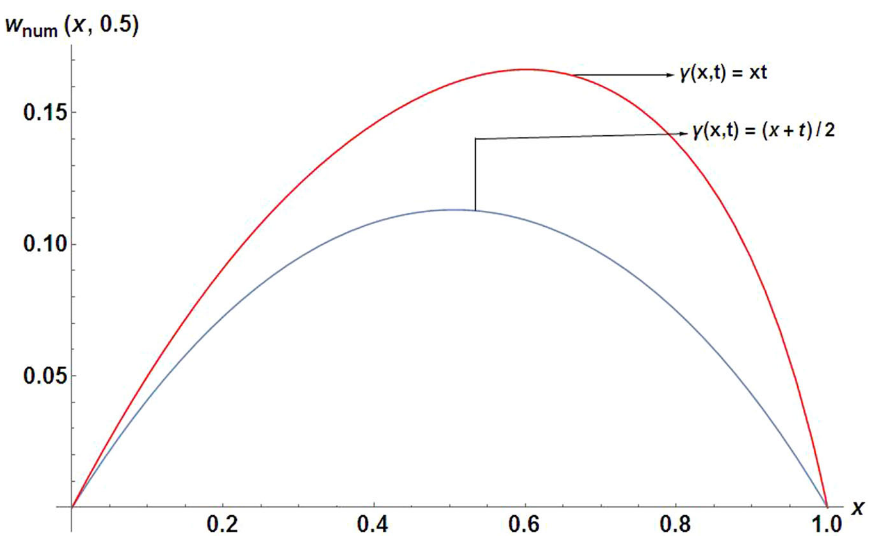

FIGURE 14 Plots of $w(x, 0.5)$ with $\lambda = 0, \delta = 1, D_1 = 1, V_1 = 0$ and $\gamma(x, t) = xt$ and $(x + t)/2$ at fixed $t = 0.5$

7 | CONCLUSION

To solve the non-linear space-time variable-order reaction–advection–diffusion equation, the shifted Legendre collocation method is applied by using operational matrices for integration, partial derivative and variable-order fractional derivative. The efficiency of the proposed model is validated by comparing the results obtained by the proposed method with the existing analytical results through error analysis. The effects of advection and reaction terms on the solution profile with different values of space and time variable-order derivative have been presented graphically. The main point of observation in this article is that the diffusivity of solute concentration is directly proportional to the non-linearity of the variable-order derivative.

ACKNOWLEDGEMENT

The authors are extending their heartfelt thanks to the reviewers for their constructive comments and suggestions to improve the quality of the revised article. The second author Subir Das acknowledges the project grant provided by Board of Research in Nuclear Sciences (BRNS), BARC, Government of India (sanction no. 58/14/07/2022-BRNS/37041).

ORCID

Chetna Biswas https://orcid.org/0000-0002-0215-0956
Subir Das https://orcid.org/0000-0002-9540-2883
Anup Singh https://orcid.org/0000-0002-6176-4931
Holm Altenbach https://orcid.org/0000-0003-3502-9324

REFERENCES

[1] Manimaran, J., Shangerganesh, L., Debbouche, A.: Finite element error analysis of a time-fractional nonlocal diffusion equation with the Dirichlet energy. J. Comput. Appl. Math. 382, 113066 (2021)
[2] Yue, C., Zhao, L.: Strong convergence of the split-step backward euler method for stochastic delay differential equations with a nonlinear diffusion coefficient. J. Comput. Appl. Math. 382, 113087 (2021)
[3] Alkhidhr, H., Jiang, Q.: Correspondence between multiwavelet shrinkage and nonlinear diffusion. J. Comput. Appl. Math. 382, 113074 (2021)
[4] Jüngel, A.: Numerical approximation of a drift-diffusion model for semiconductors with nonlinear diffusion. Z. Angew. Math. Mech. 75(10), 783–799 (1995)
[5] Křížek, M., Liu, L.: On the maximum and comparison principles for a steady-state nonlinear heat conduction problem. Z. Angew. Math. Mech. 83(8), 559–563 (2003)
[6] Bejček, M., Feistauer, M., Gallouët, T., Hájek, J., Herbin, R.: Combined triangular FV-triangular FE method for nonlinear convection-diffusion problems. Z. Angew. Math. Mech. 87(7), 499–517 (2007)
[7] Blanc, X., Labourasse, E.: A positive scheme for diffusion problems on deformed meshes. Z. Angew. Math. Mech. 96(6), 660–680 (2016)
[8] Leszczyński, H.: Finite difference schemes for a non-linear heat equation with functional dependence. Z. Angew. Math. Mech. 79(1), 53–64 (1999)
[9] Tabata, M., Eshima, N.: The Cauchy problem for the nonlinear integro-partial differential equation in quantitative sociodynamics. Appl. Math. Comput. 132(2-3), 537–552 (2002)
[10] Abergel, F., Tachet, R.: A nonlinear partial integro-differential equation from mathematical finance. Discrete Contin. Dynam. Syst.-Ser. A 27(3), 907–917 (2010)
[11] Sachs, E.W., Strauss, A.: Efficient solution of a partial integro-differential equation in finance. Appl. Numer. Math. 58(11), 1687–1703 (2008)
[12] Avazzadeh, Z., Heydari, M.H., Cattani, C.: Legendre wavelets for fractional partial integro-differential viscoelastic equations with weakly singular kernels. Eur. Phys. J. Plus 134(7), 368 (2019)
[13] Liu, P., He, T.: Dynamic analysis to the fractional order thermoelastic problem of porous structure. Z. Angew. Math. Mech. e202100251 (2022)
[14] Heydari, M.H., Avazzadeh, Z.: Legendre wavelets optimization method for variable-order fractional Poisson equation. Chaos, Solitons Fractals 112, 180–190 (2018)
[15] Hosseininia, M., Heydari, M.H., Avazzadeh, Z., Ghaini, F.M.M.: Two-dimensional Legendre wavelets for solving variable-order fractional nonlinear advection-diffusion equation with variable coefficients. Int. J. Nonlinear Sci. Numer. Simul. 19(7-8), 793–802 (2018)
[16] Singh, A., Das, S., Ong, S.H., Jafari, H.: Numerical solution of nonlinear reaction–advection–diffusion equation. J. Comput. Nonlinear Dyn. 14(4), 041003 (2019)
[17] Das, S., Singh, A., Ong, S.H.: Numerical solution of fractional order advection-reaction-diffusion equation. Therm. Sci. 22, 34 (2018)
[18] Singh, A., Das, S.: Study and analysis of spatial-time nonlinear fractional-order reaction-advection-diffusion equation. J. Porous Media 22(7), 787–798 (2019)
[19] Das, S.: Analytical solution of a fractional diffusion equation by variational iteration method. Comput. Math. Appl. 57(3), 483–487 (2009)

[20] Samko, S.G., Ross, B.: Integration and differentiation to a variable fractional order. Integral Transforms and Special Funct. 1(4), 277–300 (1993)
[21] Lorenzo, C.F., Hartley, T.T.: Initialization, conceptualization, and application in the generalized (fractional) calculus. Crit. Rev. Biomed. Eng. 35(6), 447–553 (2007)
[22] Coimbra, C.F.M.: Mechanics with variable-order differential operators. Ann. Phys. 12(11-12), 692–703 (2003)
[23] Lin, R., Liu, F., Anh, V., Turner, I.: Stability and convergence of a new explicit finite-difference approximation for the variable-order nonlinear fractional diffusion equation. Appl. Math. Comput. 212(2), 435–445 (2009)
[24] Das, S., Vishal, K., Gupta, P.: Solution of the nonlinear fractional diffusion equation with absorbent term and external force. Appl. Math. Modell. 35(8), 3970–3979 (2011)
[25] Farid, G., Latif, N., Anwar, M., Imran, A., Ozair, M., Nawaz, M.: On applications of Caputo k-fractional derivatives. Adv. Differ. Equ. 2019(1), 1–16 (2019)
[26] Almeida, R.: A caputo fractional derivative of a function with respect to another function. Commun. Nonlinear Sci. Numer. Simul. 44, 460–481 (2017)
[27] Li, C., Qian, D., Chen, Y.: On Riemann–Liouville and Caputo derivatives. Discrete Dyn. Nat. Soc. 2011, 562494 (2011)
[28] Tavares, D., Almeida, R., Torres, D.F.M.: Caputo derivatives of fractional variable order: numerical approximations. Commun. Nonlinear Sci. Numer. Simul. 35, 69–87 (2016)
[29] Shen, S., Liu, F., Chen, J., Turner, I., Anh, V.: Numerical techniques for the variable order time fractional diffusion equation. Appl. Math. Comput. 218(22), 10861–10870 (2012)
[30] Ray, S.: A new approach by two-dimensional wavelets operational matrix method for solving variable-order fractional partial integro-differential equations. Numer. Methods Partial Differ. Equ. 37(1), 341–359 (2021)
[31] Abualrub, T., Sadek, I.: Legendre wavelet operational matrix of derivative for optimal control in a convective–diffusive fluid problem. J. Frankl. Inst. 351(2), 682–693 (2014)
[32] Razzaghi, M., Yousefi, S.: The Legendre wavelets operational matrix of integration. Int. J. Syst. Sci. 32(4), 495–502 (2001)
[33] Dehestani, H., Ordokhani, Y., Razzaghi, M.: Pseudo-operational matrix method for the solution of variable-order fractional partial integro-differential equations. Eng. Comput. 37(3), 1791–1806 (2021)

How to cite this article: Biswas, C., Das, S., Singh, A., Altenbach, H.: Solution of variable-order partial integro-differential equation using Legendre wavelet approximation and operational matrices. Z Angew Math Mech. e202200222 (2022). https://doi.org/10.1002/zamm.202200222